Proceedings of the IEEE International
Conference on Robotics and Automation
May 2015 Seattle, WA, USA

Operation of the Ballbot on Slopes and with Center-of-Mass Offsets

Bhaskar Vaidya, Michael Shomin, Ralph Hollis, and George Kantor

***Abstract*— The ballbot is a human sized, dynamically stable mobile robot that balances on a single, spherical wheel. The current framework for navigation and control makes the assumption that the robot is operating on a level surface without any center-of-mass offset; however, in practice, such a dynamically stable robot has to be able to successfully navigate sloped surfaces and with such offsets. This work develops the equations of motion for the ballbot system on a sloped surface with a center-of-mass offset. The equilibria of this system are analyzed, and a compensation strategy is formulated that allows the ballbot to operate in the presence of slopes and center-of-mass offsets. This work also develops estimation algorithms for slope and center-of-mass offset angles during station-keeping and trajectory following. Results for compensation and estimation are demonstrated experimentally.**

I. INTRODUCTION

The ballbot is a dynamically-stable mobile robot that actively balances on a single, spherical wheel. It was designed to be roughly the height and weight of a human and is capable of omnidirectional motion, which makes it suited to operating in human environments. Dynamic balancing also affords the robot inherent compliance; it can be physically handled and pushed hard without going unstable. This compliance makes the ballbot a good candidate for exploring human-robot interaction. The system also contains two simple, two degree-of-freedom arms that allow for rudimentary manipulation. A complete description of the ballbot system can be found in [1].

In prior work, a number of capabilities such as balancing [2], station keeping [3], trajectory following [4], and path planning [5] have been developed to enable autonomous navigation on level floors. The robot accelerates by leaning, and can execute lean-angle trajectories to produce desired motion in position space. However, the planning and control architecture in the earlier work was not designed to operate on sloped floors or when the system has a significant center of mass offset.

Consideration of non-zero floor slopes and center-of-mass (COM) offsets is essential to furthering the capabilities of the ballbot. Human environments do not only consist of level floors, but include sloped floors that are often in critical locations (*e.g.*, accessibility ramps). Additionally, carrying objects with unknown mass using the system's arms will result in an unknown center-of-mass of the system.

This work was supported by NSF CMMI grant 1234589

Bhaskar Vaidya is a Master's Candidate at the Robotics Institute, Carnegie Mellon University, Pittsburgh, PA 15213, USA bvaidya@andrew.cmu.edu

Michael Shomin is a PhD Candidate, also at the Robotics Institute mshomin@cmu.edu

Ralph Hollis is a Research Professor, also at the Robotics Institute rhollis@cs.cmu.edu

George Kantor is a Senior Systems Scientist, also at the Robotics Institute kantor@cmu.edu

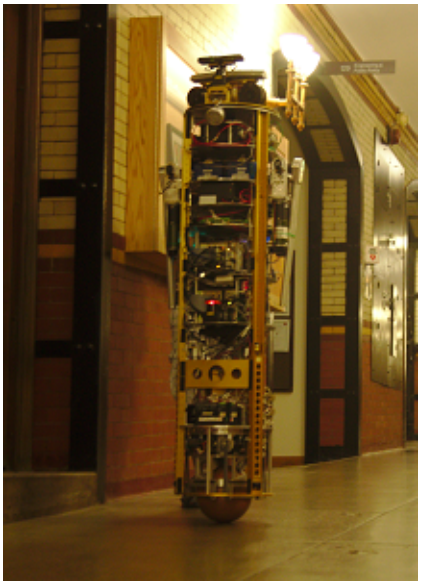

Fig. 1: The ballbot, a dynamically balancing mobile robot, operating on a sloped surface.

To our knowledge, this problem has not been directly addressed for a ballbot before, however some relevant work has been done for the closely related mobile wheeled inverted pendulum (MWIP) personal vehicles such as the Segway RMP220 and the AIST Japan PMP [6]. For example, Takei *et al.* have developed a Luenberger estimator to simultaneously estimate the floor slope and human-imparted forces in the period during which a human is disembarking from the PMP [7]. The resulting estimate was experimentally validated and shown to be accurate to within 1° on a 9° slope, and was sufficient to be used in a position controller that would keep the vehicle from rolling down the slope after the rider let go. Hirata *et al.* developed a reaction torque observer to estimate the effect of slope angles on a two-wheeled wheelchair, and used those estimates in a second order controller to stabilize the wheelchair on 5° slopes [8]. Huang *et al.* also investigated the problem of operating a MWIP on sloped floors [9], but they bypassed the estimation problem in favor of creating a sliding-mode velocity controller designed to be robust to floor slope. The resulting controller was shown in simulation to successfully stabilize the system for constant, unknown slopes ranging from -5° to $+5^\circ$, however the closed loop system exhibited undesirable slope-dependent steady state errors. Key *et al.* also explored solving the problem of operating a two-wheeled inverted pendulum on slopes using a sliding mode controller in simulation [10].

This paper takes a pragmatic approach to estimating and compensating for both the floor slope and the center of

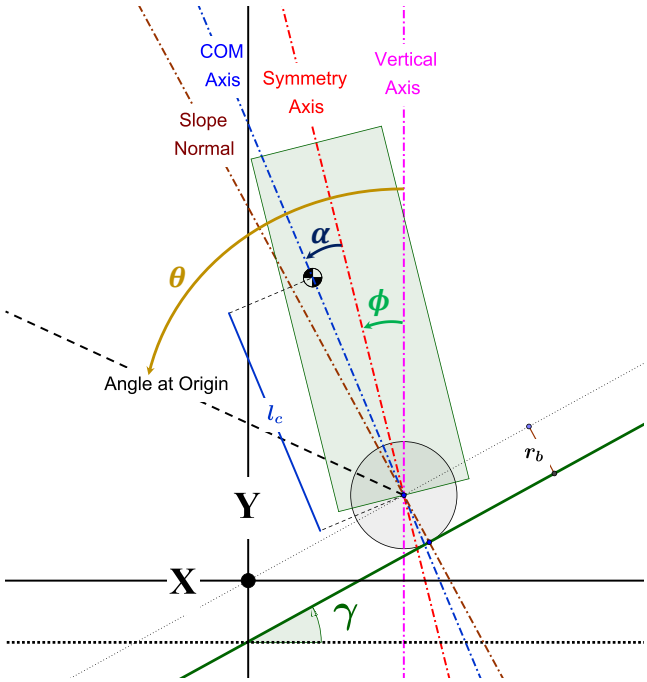

Fig. 2: The planar ballbot model, including a non-zero slope and center-of-mass offset angle.

mass offset of the ballbot during autonomous operation. This paper first develops the equations of motion for the ballbot on a slope and with non-zero COM offset. Based on analysis of the resulting equilibrium conditions, a feed-forward strategy that compensates for known slopes and COM offsets is proposed and shown to eliminate steady state error in the ballbot position controller. To handle the case where floor slope and COM offset are unknown, strategies for online estimation of the necessary compensation angle are proposed for station-keeping and trajectory-following cases. These strategies have been implemented on the ballbot and validated experimentally.

II. MODELING AND ANALYSIS

In order to understand the effects that the addition of a non-zero floor slope and center-of-mass offset angle have on the ballbot system, the equations of motion are derived using the Lagrangian method. As in prior work, the decoupled planar model of the ballbot is used [2].

The parameters of this model are shown in Fig. 2. The floor slope γ is defined as the angle between the horizontal and the floor, where a positive γ implies that the height of the floor *decreases* in the positive **X** direction. Correspondingly, the center-of-mass offset angle α is defined as the angle between the axis of symmetry of the ballbot and the axis connecting the center of the ball and the center of mass of the ballbot body. A positive α leans the center of mass of the body in the positive **X** direction (for angles under $\frac{\pi}{2}$). The complete set of system parameters are given in Table I. The equations of motion for the system are computed as follows:

$$\begin{bmatrix}\tau\\0\end{bmatrix} = M\begin{bmatrix}\ddot{\theta}\\\ddot{\phi}\end{bmatrix} + C\begin{bmatrix}\dot{\theta}\\\dot{\phi}\end{bmatrix} + G\,, \tag{1}$$

where

$$M = \begin{bmatrix} a & b\cos(\gamma-\phi-\alpha) \\ a + b\cos(\gamma-\phi-\alpha) & c + b\cos(\gamma-\phi-\alpha)\end{bmatrix},$$
$$C = \begin{bmatrix} 0 & -b\sin(\gamma-\phi-\alpha)\,\dot{\phi} \\ 0 & -b\sin(\gamma-\phi-\alpha)\,\dot{\phi}\end{bmatrix},$$
$$G = \begin{bmatrix} -d\sin(\gamma) \\ -d\sin(\gamma) - g\,l_c\,m_B\sin(\alpha+\phi)\end{bmatrix},$$

with:

$$\begin{aligned} a &= r^2\,(m_B + m_b) + I_b,\\ b &= r\,l_c\,m_B,\\ c &= I_B + {l_c}^2\,m_B,\\ d &= g\,r\,(m_B + m_b)\,. \end{aligned}$$

Note that in this representation of the system, the equations of motion have been transformed to make the second equation unforced. The canonical state-space representation of the ballbot system can then be constructed as follows:

$$x = \begin{bmatrix}\theta\\\phi\\\dot{\theta}\\\dot{\phi}\end{bmatrix}, \qquad \dot{x} = \begin{bmatrix}\dot{\theta}\\\dot{\phi}\\f_1\\f_2\end{bmatrix}, \tag{2}$$

where

$$\begin{aligned} f_1 = \frac{1}{a\,c - b^2\,\cos^2(\gamma-\phi-\alpha)}\Big(&c\,\tau + b\,\tau\,\cos(\gamma-\phi-\alpha)\\ &+ b\,c\,\sin(\gamma-\phi-\alpha)\,\dot{\phi}^2 + c\,d\,\sin(\gamma)\\ &- b\,g\,l_c\,m_B\,\sin(\alpha+\phi)\,\cos(\gamma-\phi-\alpha)\Big), \end{aligned}$$

$$\begin{aligned} f_2 = \frac{1}{a\,c - b^2\,\cos^2(\gamma-\phi-\alpha)}\Big(&a\,g\,l_c\,m_B\,\sin(\alpha+\phi)\\ &- b\,d\,\sin(\gamma)\cos(\gamma-\phi-\alpha) - a\,\tau\\ &- b^2\,\sin(\gamma-\phi-\alpha)\cos(\gamma-\phi-\alpha)\,\dot{\phi}^2\Big). \end{aligned}$$

In order to characterize the effect of a non-zero floor slope and center-of-mass offset angle on the ballbot system, the equilibrium conditions of (2) are calculated by setting $\dot{x}$

TABLE I: Model Configuration Variables and Parameters

ϕ	Lean angle (w.r.t vertical axis)
θ	Ball angle (arc length of ball traversal))
α	Center of mass offset (w.r.t. symmetry axis)
γ	Slope angle (w.r.t. horizontal axis)
l_c	Distance from ball center to center of mass of body
r	Ball radius
m_b	Ball mass
m_B	Body mass
I_b	Ball inertia
I_B	Body inertia

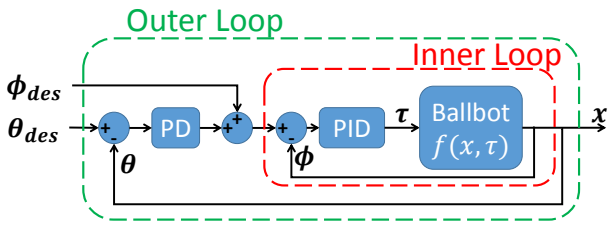

Fig. 3: Nested ballbot PID controller

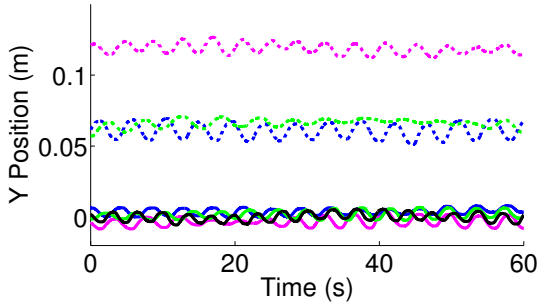

Fig. 4: Comparison of ball position responses with (shown with solid lines) and without (shown with dotted lines) feed-forward compensation in the presence of center-of-mass offsets. The colors represent different center-of-mass offset angles- Black: $0°$, Green: $0.28°$, Blue: $0.31°$, Magenta: $0.55°$.

equal to zero and solving for the resulting equilibrium lean angle ϕ_{eq} and input torque τ_{eq}:

$$\phi_{eq} = \sin^{-1} \frac{-r \, \sin(\gamma) \, (m_b + m_B)}{l_c \, m_B} - \alpha, \tag{3}$$

$$\tau_{eq} = -d \, \sin(\gamma) \, . \tag{4}$$

When the slope angle γ and the center-of-mass angle α are zero, the equilibrium lean angle ϕ_{eq} and input torque τ_{eq} are zero. When $\gamma = 0$, a non-zero center-of-mass offset angle α will result in an equilibrium lean angle of $\phi_{eq} = -\alpha$. In the presence of a non-zero slope angle γ, the equilibrium lean angle leans farther into the slope in because the center-of-mass of the ball is no longer above the point of contact between the ball and the floor. Additionally, the system also has to exert a non-zero torque between the ball and the body to prevent the ball from rolling down the slope.

III. CLOSED LOOP RESPONSE AND COMPENSATION

This shift in equilibrium caused by the slope angle γ and the center-of-mass offset angle α affects the operation of the ballbot while running the ballbot position controller. This controller consists of a nested PID architecture, as described in [4]. The inner loop of this controller tracks a lean-angle command by actuating the ball, while the outer loop tracks the ball position on the floor and feeds lean-angle setpoints to the inner loop controller, as shown in Fig. 3.

A. Center-of-Mass Offsets

In order to determine the effect of operating this controller with a non-zero center-of-mass offset angle α, three experiments were performed. Non-zero α were induced in the y-axis of the robot by placing different masses at a known location on the second-top deck of the robot. For offset angles of $0.28°$, $0.31°$, and $0.55°$, as well a control with no center-of-mass offset angle, the ballbot was commanded to hold a specific position on the floor (station-keeping) by commanding a constant position to the PD outer loop controller. The y-axis position data of the ball were collected over all of the experiments. A comparison of the desired and actual y-axis ball position values is shown (dotted lines) in Fig. 4. In each trial, the ball response is oscillatory about a steady-state value, due to the fact that the ballbot is attempting to maintain an unstable equilibrium. The non-zero center-of-mass offsets cause a steady-state error in the steady-state position of the ballbot relative to the desired position, increasing with the angle of the offset. Thus, in the presence of non-zero α, the controller configuration shown in (3) exhibits steady-state error in tracking outer-loop position commands.

Despite the small magnitudes of the steady-state offsets in both cases ($\alpha \neq 0$, $\gamma \neq 0$), any systemic steady-state offset breaks the assumptions that higher level navigation planners may make about the closed-loop operation. While the position controller could utilize an integral term in the outer loop to mitigate this steady-state offset, the system is subject to frequent disturbances from physical interaction with humans that would make the addition of an integral term a safety hazard.

A simple compensation strategy can be implemented that improves the controller's performance in the presence of non-zero floor slope angles and center-of-mass offsets. The existing controller was designed under the assumption of level floor and no center-of-mass offset; in order to incorporate the effect of α (and γ) on the equilibrium of the system, the equilibrium lean angular value (3) and equilibrium torque value (4) can be fed-forward into the existing controller architecture, as shown in Fig. 5. Intuitively, this approach simply shifts the old control inputs, at both inner and outer loop control level, to operate about the actual equilibrium, instead of a zero equilibrium. Practically, the feed-forward equilibrium torque is not needed, due to the fact that the inner loop controller is a PID controller with an integral term. As long as the feed-forward equilibrium lean angle is correct, the output torque will quickly converge to the equilibrium torque. Thus, the modified controller only requires the feed-forward equilibrium lean angular term.

In order to evaluate the performance of the modified controller in the presence of non-zero α, the same COM offset angles ($0.28°$, $0.31°$, and $0.55°$) were induced in the system. The ballbot was then commanded to station-keep about a specific position on the floor, and the ball position data were collected as before. The differences between the desired and actual ball positions using the modified controller are also shown in Fig. 4 (solid lines). With the modification to the controller, errors in ball position in all three trials are clustered around zero, just as in the control test with no COM offset angle. Thus, the modified controller fixes the non-ideal behavior of the ballbot in the presence of COM offsets.

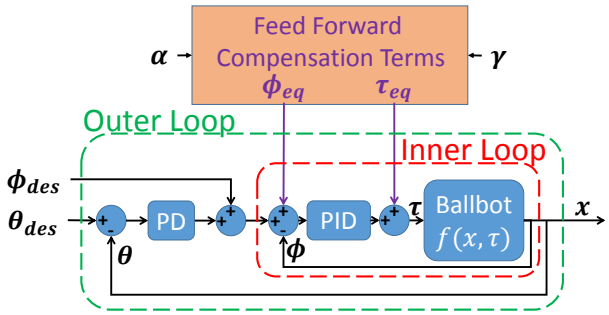

Fig. 5: Modified ballbot controller incorporating feed-forward compensation.

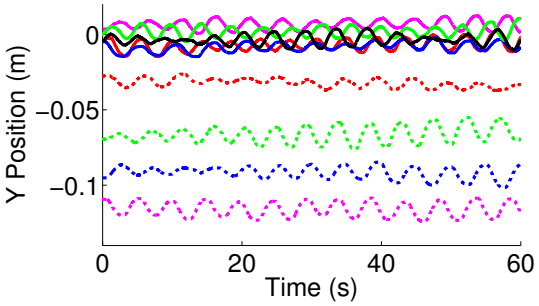

Fig. 7: Comparison of ball position responses with (shown with solid lines) and without (shown with dotted lines) feed-forward compensation in the presence of floor slopes. The colors represent different floor slopes- Black: 0°, Red: 1°, Green: 2°, Blue: 3°, Magenta: 4°

B. Floor Slopes

Similar experiments were conducted to evaluate the improvement in the operation of the robot on sloped surfaces when using the modified controller. These tests were conducted on a variable slope ramp, shown in Fig. 6. The ramp was adjusted to angles γ of roughly 1°, 2°, 3°, and 4° for the different tests. A control experiment was also run on level floor. In each test, the ballbot was commanded to hold a specific position on the ramp, using the outer loop PD controller. For the first set of four tests, each with a different γ, the ballbot utilized the original controller (Fig. 3); for the second set, the controller modification was added (Fig. 5). The ramp was aligned with the y-axis of the robot; thus, only the y-axis plane of the robot was directly affected by the floor slope. Steady-state y-axis ball position data were collected over all eight trials (Fig. 7). When using the original controller without the feed-forward modification, the error between the desired and actual ball positions increases with increasing slope (dotted lines); however, the addition of feed-forward equilibrium lean-angle compensation eliminates this error for all of the slope angles (solid lines). Using this controller modification, the ballbot is able to satisfactorily track input position commands in the presence of both non-zero center-of-mass offset angles α and slope angles γ.

IV. ESTIMATION

The feed-forward compensation method utilized in the modified controller (Fig. 5) assumes full knowledge of the floor slope angle γ and center-of-mass offset angle α. However, it is often the case that these values are unknown or changing; thus, some sort of estimation is required in order to operate the modified controller. If the equilibrium lean angle can be estimated, the modified controller can be successfully run, as the equilibrium torque value is not needed. The following methods estimate the equilibrium lean angles arising from center-of-mass offsets and slopes separately; while the two are coupled, the foreseen use cases for the robot only necessitate having to estimate only one component at a time.

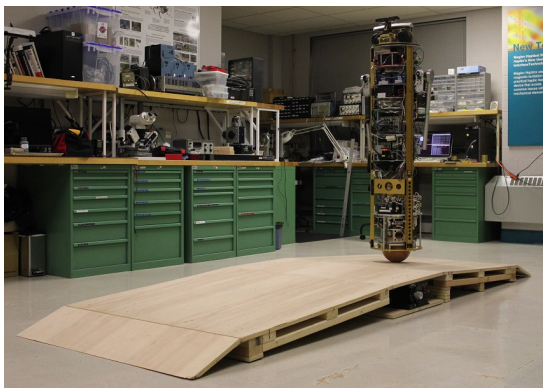

Fig. 6: The ballbot station-keeping on a variable-slope ramp.

A. Station-keeping

When the robot attempts to maintain a specific position in the world using the outer loop position tracking controller (station-keeping), it oscillates about some steady-state position as seen in Fig. 7. The average lean angle during station-keeping is therefore the equilibrium lean angle of the robot since the robot has no net velocity or acceleration over the oscillation period. This results in a simple strategy to extract the equilibrium lean angle of the robot: enable station-keeping and average the lean angle over some period of time. To verify that this method works, several tests were run.

This strategy was implemented for the ballbot and tested experimentally. In the first set of experiments, center-of-mass offset angles were induced as described earlier (0.28°, 0.31°, and 0.55° in the y-axis). The robot was commanded to hold a position on the floor for 5 s (the period of oscillation), and y-axis lean angular data were averaged over that duration to obtain an estimate for the equilibrium lean angle. Because the floor slope angle γ was zero, the center-of-mass offset angle α could be calculated using (3). The estimated values of α are compared to the actual values in Fig. 8. The center-of-mass offset angle can be reliably estimated to within 0.05° using this method.

In the second set of experiments, the robot was commanded to station-keep on the variable slope ramp for 5 s. The ramp was adjusted to roughly 1°, 2°, 3°, and 4° in each of the four experiments. The ramp was aligned with the y-axis of the robot, so that only that axis would be affected by the slope. The y-axis lean angular data were averaged over the duration of the experiment to obtain an estimate for the equilibrium lean angle. Because the center-of-mass offset

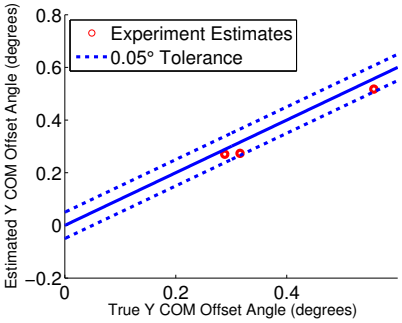

Fig. 8: Comparison of estimated and actual center-of-mass offsets while station-keeping.

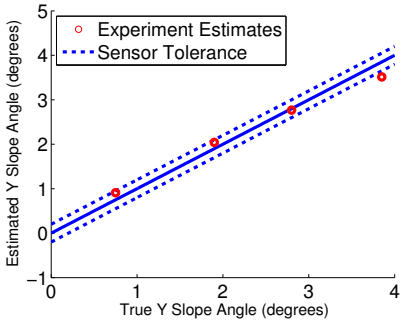

Fig. 9: Comparison of estimated and actual slope angles while station-keeping.

angle α was zero, the slope angle γ could be calculated from the equilibrium lean angle using (3). The estimated values of the slope angle γ are compared to the actual values in Fig. 9. The slope angle can be estimated to within the tolerance of the sensor used to measure the ground truth value ($0.2°$).

B. Trajectory Following

While this method of station-keeping to determine the equilibrium lean angle is effective, it is limiting because the robot is constrained to hold a single position while estimating. A more effective estimator would be able to estimate the equilibrium lean angle of the robot while executing arbitrary dynamically-feasible motions.

The ballbot internal dynamics provide the basis for such an estimator. They are given by the unforced equation of motion in (1), which can be written out as

$$\begin{aligned} 0 = &\big(a + b\,\cos(\gamma - \phi - \alpha)\big)\,\ddot{\theta} \\ &+ \big(c + b\,\cos(\gamma - \phi - \alpha)\big)\,\ddot{\phi} \\ &- b\,\sin(\gamma - \phi - \alpha)\,\dot{\phi}^2 - d\,\sin(\gamma) \\ &- g\,l_c\,m_B\,\sin(\alpha + \phi). \end{aligned}$$

This equation can be simplified by making the small angle assumption for the lean angle ϕ, the slope angle γ, and the center-of-mass offset angle α. The $\dot{\phi}^2$ term has been experimentally observed to be negligible in practice, and is approximated as zero. The resulting approximate internal dynamics can be written as

$$\frac{r\,(m_b + m_B)\,\gamma}{l_c\,m_B} + \alpha = \frac{(a+b)\,\ddot{\theta}}{g\,l_c\,m_B} + \frac{(c+b)\,\ddot{\phi}}{g\,l_c\,m_B} - \phi\,. \quad (5)$$

At this point, we introduce the equilibrium lean angle estimator as

$$\hat{\phi_{eq}} = -\frac{(a+b)\,\ddot{\theta}}{g\,l_c\,m_B} - \frac{(c+b)\,\ddot{\phi}}{g\,l_c\,m_B} + \phi\,. \quad (6)$$

By combining (5) and (6), we notice that

$$\hat{\phi_{eq}} = -\frac{r\,(m_B + m_b)\,\gamma}{l_c\,m_B} - \alpha\,.$$

This estimator output $\hat{\phi_{eq}}$ is thus equal to the small angle approximation of the equilibrium lean angle given in (3); as such, because the ballbot is operating in the small-angle regime, this estimator output should be very close to the actual value of ϕ_{eq}.

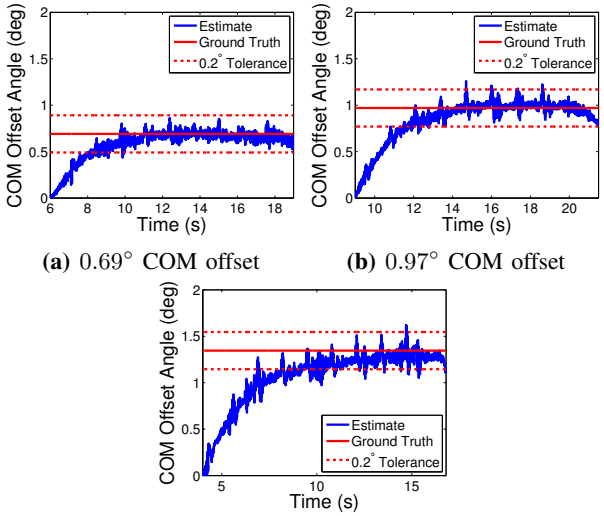

(a) $0.69°$ COM offset **(b)** $0.97°$ COM offset

(c) $1.35°$ COM offset

Fig. 10: Estimation of COM offset during dynamic motion.

This estimator requires knowledge of the ball angular acceleration $\ddot{\theta}$ and lean angular acceleration $\ddot{\phi}$. The accelerations are not directly measured, so they are estimated through a combination of single-sided finite differencing of the measured velocities $\dot{\theta}$ and $\dot{\phi}$ with a first order low pass filter to reduce the resulting noise. The output of this filter is taken as the current approximation to the equilibrium lean angle. The equilibrium lean angle captures the effects of both the floor slope angle γ and the center-of-mass offset angle α; thus, it is sufficient to estimate this quantity alone.

In order to demonstrate that the estimator (6) could accurately identify the equilibrium lean angle of the robot while executing dynamic trajectories, several experiments were performed. In the first set of experiments, center-of-mass offsets were induced in the y-axis of the robot by moving the arms to an offset angle in front of the body. In this way, α values of $0.69°$, $0.97°$, and $1.35°$ were generated in the system. The robot was commanded to execute dynamically feasible trajectories [11] across the room, and the estimator was started at the beginning of each trajectory. Time series of the estimator output for each of the trial cases are plotted in Fig. 10. The estimator converges to within $0.2°$ of ground truth within 10 s for all three experiments.

Similarly, tests were run in order to demonstrate the

performance of the estimator on sloped surfaces. In these experiments, the center-of-mass offset of the system was manually compensated for, and thus assumed to be zero. The robot executed trajectories across a hallway that transitioned from a roughly level floor to a sloped floor of 3° (Fig. 1), in order to determine if the estimator could accurately discriminate the transition between the level and sloped portions of the floor. The results of these experiments are shown in Fig. 11. In both experiments, the estimate first converges to the initial slope angle, and then transitions to the new slope angle as the ballbot travels across the division and onto the new slope. The estimator converges to within a low tolerance of the ground truth equilibrium lean-angular value within a span of 10 s.

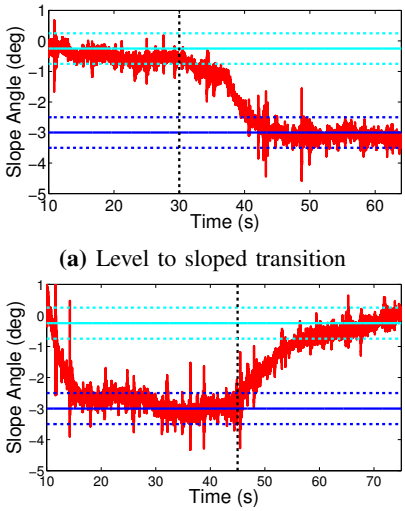

(a) Level to sloped transition

(b) Sloped to level transition

Fig. 11: Estimation of slope angle during dynamic motion. The cyan lines indicate a floor slope of $-0.25°$ (flat floor). The blue lines indicate a floor slope of $-3°$. The estimator output is shown in red, and the vertical dotted black line indicates the time of transition between slope angle values.

V. CONCLUSIONS AND FUTURE WORK

A feed-forward method of compensating for the effect of floor slopes and center-of-mass offsets on the ballbot system has been presented. This strategy allows the ballbot to operate on sloped floors and with center-of-mass offsets in the same way it does on level floors with no offset. Experimental results showing the improvement in performance under different α, γ demonstrate the viability of this method. Additionally, an estimator is presented that is able to accurately estimate floor slope angles γ and center-of-mass offset angles α within 10 s. These are important modifications furthering the capability of the ballbot system.

The separate methods for estimating and compensating for floor slopes and COM offsets outlined in this paper can in the future be integrated to form a closed loop system that can adapt to changes in these parameters. Further work can be done to remove some of the high-frequency noise present in the angle estimates. Further experimentation can also be conducted to investigate the accuracy of the techniques presented while the ballbot is yawing on a slope, as there are minor unmodeled dynamics that may affect performance. As the ballbot will be physically interacting with humans in the future, care needs to be taken regarding the effects of such unmodeled dynamics on the estimator output. Additionally, the speed of estimate convergence may be increased by considering more sophisticated estimation techniques.

REFERENCES

[1] Umashankar Nagarajan, George Kantor, and Ralph Hollis. The ballbot: An omnidirectional balancing mobile robot. *Int'l. J. of Robotics Research (IJRR)*, 33:917–930, 2013.

[2] Tom Lauwers, George Kantor, and Ralps Hollis. One is enough! In *Proc. Int'l. Symp. for Robotics Research*, 2005.

[3] T. B. Lauwers, G. A. Kantor, and R. L. Hollis. A dynamically stable single-wheeled mobile robot with inverse mouse-ball drive. In *Proc. IEEE Int'l. Conf. on Robotics and Automation*, pages 2884–2889, 2006.

[4] Umashankar Nagarajan. *Fast and Graceful Balancing Mobile Robots*. PhD thesis, Carnegie Mellon University, The Robotics Institute, 2012.

[5] Michael Shomin and Ralph Hollis. Fast, dynamic trajectory planning for a dynamically stable mobile robot. In *IEEE/RSJ International Conference on Intelligent Robots and Systems (TO APPEAR)*, 2014.

[6] Makiko Sasaki, Naoto Yanagihara, Osamu Matsumoto, and Kiyoshi Komoriya. Steering control of the personal riding-type wheeled mobile platform (PMP). In *Intelligent Robots and Systems, 2005.(IROS 2005). 2005 IEEE/RSJ International Conference on*, pages 1697–1702. IEEE, 2005.

[7] Toshinobu Takei, Osamu Matsumoto, and Kiyoshi Komoriya. Simultaneous estimation of slope angle and handling force when getting on and off a human-riding wheeled inverted pendulum vehicle. In *Intelligent Robots and Systems, 2009. IROS 2009. IEEE/RSJ International Conference on*, pages 4553–4558. IEEE, 2009.

[8] Kazuya Hirata, Miyuki Kamatani, and Toshiyuki Murakami. Advanced motion control of two-wheel wheelchair for slope environment. In *IEEE Industrial Electronics Society*, pages 6436–6441, 2013.

[9] Jian Huang, Zhi-Hong Guan, Takayuki Matsuno, Toshio Fukuda, and Kosuke Sekiyama. Sliding-mode velocity control of mobile-wheeled inverted-pendulum systems. *Robotics, IEEE Transactions on*, 26(4):750–758, 2010.

[10] Min-Sun Key, Chang-Gook Jeon, and Dong Sang Yoo. Sliding mode control for a two-wheeled inverted pendulum mobile robot driving on uniform slopes. In *International Conference on Control, Automation and Systems*, pages 2159–2162, 2012.

[11] Michael Shomin and Ralph Hollis. Differentially flat trajectory generation for a dynamically stable mobile robot. In *IEEE Int'l. Conf. on Robotics and Automation*, pages 2373–2377, 2013.